Selectively convert fructose to furfural or hydroxymethylfurfural on Beta zeolite: The manipulation of solvent effects

Yueqing Wang[a,b], Guoqiang Ding[c], Xiaohai Yang[a,b], Hongyan Zheng[c], Yulei Zhu[a,c,*], Yongwang Li[a,c]

[a] State Key Laboratory of Coal Conversion, Institute of Coal Chemistry, Chinese Academy of Sciences, Taiyuan, 030001, PR China
[b] University of Chinese Academy of Sciences, Beijing, 100049, PR China
[c] Synfuels China Co. Ltd., Beijing, PR China

A B S T R A C T

The selective synthesis of furfural or hydroxymethylfurfural (HMF) from fructose on single catalyst (Beta zeolite, Hβ) is challenging task. However, in this study, selectivity of Hβ zeolite was discovered easily to tune by solvent effects. Strong solvent effects on the selectivity of fructose conversion were observed in different manners depending on the solvent used. It was shown that the coordinated state of framework aluminum, induced by solvent effects, has a major impact on the selectivity. The solvents with amide group were discovered to induce the reversible tetrahedral-octahedral framework aluminum transformation, but the configuration of aluminum was no influenced by other solvents such as γ-butyrolactone (GBL). Compared with other solvents, the GBL was not able to enhance turnover frequency (TOF) value of reaction but also suppress the degradation of furfural. Interestingly, a considerable yield of furfural (50.25%) was obtained combined with tetrahedral and octahedral framework aluminum active sites in GBL, while high selectivity of HMF (83.3%) was achieved in presence of single tetrahedral framework aluminum over Hβ in NMP.

1. Introduction

The depletion of petroleum, climate change and growing concerns about energy and environmental issues urged our society to seek for clear and renewable sources. Biomass resources are particularly attractive as an alternative to fossil resources for the production of chemicals and fuels due to its abundance, sustainability and wide distribution in nature [1,2]. The major components of plant-derived biomass are carbohydrate, and these are recently viewed as a renewable feedstock for the synthesis of platform compounds. Among the products that can be obtained from sugars, furfural and hydroxymethylfurfural (HMF) are particularly promising option. Both furfural and HMF are the most important platform chemicals that can be further upgraded to valuable fine chemicals and liquid fuels through chemocatalysis process. For example, HMF can be obtained not only from fructose but also from glucose *via* isomerization to fructose, as well as directly form cellulose. It is useful not as intermediate for the production of the biofuel dimethylfuran and other molecules, but for important value-added fine chemicals such as levulinic acid, 2,5-furandicarboxylic acid, 2,5-diformylfuran. Although a vast range of solid acid catalysts, including zeolites [3–6], acidic ion-exchange resins [7–9], heteropolyacid

salts [10–12], oxides [13–15], and sulfates[16], have been investigated in the presence of different reaction systems such as water [17], single phase [18], biphase [19], and ionic liquid (IL) [20], the industrial production of HMF is currently impeded by high costs of manufacturing. Therefore, HMF is not yet a high-volume chemical in consideration of difficulties in cost-effective production. However, furfural, which can complement oil-based organics for the production of resins, lubricants adhesives, and plastics, has been industrially produced from agricultural waste or other uneatable hemicellulose rich in pentosan using the Quaker Oats technology [2,21]. Noteworthily, world market for furfural is estimated conservatively to be about 250,000 ton per annual of which approximately 70% was used for producing furfuryl alcohol at 2008 [22]. Recently, the global demand for furfural still increasing driven by growing environment concerns. Owing to the significant importance of furfural in sustainable chemistry, in the past decade, considerable efforts have been devoted in the conversion of carbohydrates to these furan chemicals [23,24]. Typically, furfural was mainly obtained by acid catalytic conversion of five-carbon (C_5) mono- and poly-saccharides. Compared with the other solid acids, zeolites, which have a structure of crystalline sheets, attracted more attention in the production of furfural (C_5) from xylose (C_5) [25–27]. One of the

main advantages of these materials is their shape selectivity and possibility to control the pore size thus to obtain an optimal structure for intended end use. However, J. A. Dumesic group [4] found that fructose and glucose (six-carbon sugars, C_6-sugars) could be transformed into furfural (C_5) over Hβ and mordenite zeolite. Moreover, Cui et al. [28] first reported that the appropriable yield for furfural (38.5%) was obtained by the direct conversion of cellulose *via* selective the carbon-carbon bond cleavage over Hβ. Noteworthily, the cellulose is the most abundant component of lignocellulosic biomass in nature. In addition, a large amount of amorphous cellulose is produced as a residual solid in the furfural production industry, which is used as a fuel to provide steam for the plant [22]. This interesting finding established that these catalytic systems might provide a new way in the synthesis of furfural from cellulose and its derived sugars. Among all kinds of zeolites, Hβ zeolite possesses a three-dimensional intersecting channels with pore openings size of 6.6×6.7 Å [29]. The intriguing structure and chemical properties of Hβ zeolite make it an effective material in production of furfural via selective carbon-carbon bond cleavage [28]. However, the development of a single catalyst for the effective production of both furfural and HMF from C6-sugars is still challenging. Recently, we found that the selectivity of Hβ could be tuned by solvent effect (Scheme 1). Moreover, there is no yet clear picture of solvent effects on the selectivity of Hβ, as well as the catalytic performance in conversion of C_6 carbohydrates so far. Apparently, advances towards understanding solvent effects on the conversion of fructose could lay the foundations for the rational design of catalytic systems for production of furfural (C_5) or HMF (C_6) from C_6 carbohydrates.

1.1. Brief introduction of solvent effects

The solvent effect, which is a common phenomenon in homogeneous catalysis, may affect the solubility, stability and reaction rate of the reaction system. Likewise, such a solvent effect has also been observed in heterogeneous catalysis. Generally, solvents could play critical roles in determining reaction rate and selectivity of products in multitudinous of heterogeneous catalysis processes. Since the various properties of solvents can influence catalyzed reaction in many different ways, solvent effect is a complicated issue that involves solubility, mass transfer, interplay with initial materials or products, transition state stabilization and interaction with catalysts. In all these aspects, the interaction between solvent and catalysts is the most important factor. The significant influence of solvents-catalyst interaction had been widely demonstrated in numerous of studies [30–33]. For example, γ-valerolactone and tetrahydrofurans, as the polar aprotic organic solvents, can stabilize H^+ and promote the protonated transition state in dehydration of xylose over zeolite [34]. Xun Hu and Chun Zhu Li [35] also pointed that the solvents significantly affect the swelling of the acidic resin catalyst and availability of the inner acidic sites duo to their different polarities in dehydration of xylose. × .Y. Wang and Rinaldi [36] also mentioned that the activity and selectivity

of Raney Ni catalyst was significant influenced by solvent in hydrogenolysis of lignin. Additionally, V.V. Ordomsky and T.A. Nijhuis et al. proposed that the interaction between organic solvent and zeolite acid sites play an important role for improving the selectivity of HMF [37].

In this paper, we present the result of the investigation into the effect of various solvent for the conversion of fructose over Hβ. Many representative polar protic and non-protic solvents such as alcohols, γ-lactones, ethers, ketones, possessing different the properties and functional group, are employed to get insight into the solvent effect on distribution of products. In an effort to understand the solvent effect, seven solvents including isopropanol, 2-butanol, γ-butyrolactone (GBL), γ-valerolactone (GVL), 1,4-dioxane, acetone, N-methyl-pyrrolidone (NMP) have been evaluated in the acid-catalyzed conversion of fructose over the Hβ. Among all the solvents, the higher yield of furfural was obtained in GBL. On the contrary, the dehydration of fructose into HMF was predominant and only little amount of furfural in NMP. These results indicate that the catalytic performance of Hβ is strongly influenced by solvent effects. From the standpoint of solvent effects, we hypothesize that synergistic effect between solvent molecular and Hβ could result in different distribution of products.
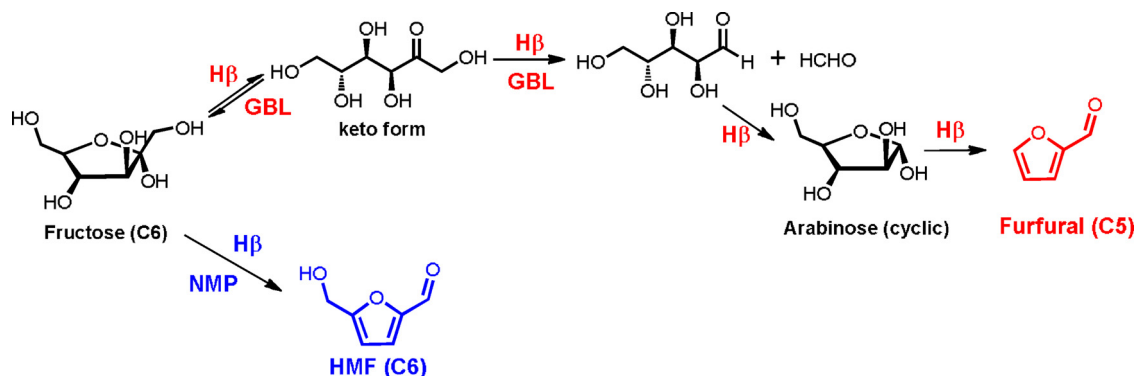
2. Experimental section

2.1. Materials

Fructose (analytical grade, 99.5%), 5-hydroxymethylfurfural (HMF, > 99.0%), furfural (≥ 99.5%), Nmethylpyrrolidone (NMP, Electronic Grade, 99.9%), 1,3-dimethyl-2-imidazolidinone (DMI, analytical grade, > 98.0%), γ-butyrolactone (GBL, chromatographic grade, 99.9%), and N,Ndimethyl acetamide (DMA, chromatographic grade, 99.8%) were obtained from Shanghai Aladdin Co., Ltd. Other solvents were purchased from Sinopharm Chemical Reagent Co.,Ltd. Hβ zeolite was purchased from Nankai University Catalyst Co., Ltd. All reagents utilized in this work were used as received without further purification.

2.2. Dehydration of fructose and analysis

All experiments were performed in a batch reactor (50 mL) with a magnetic stirrer. Typically, sugar (5 wt %) and a certain volume of the solvent were added in the vessel, followed by the addition of a catalyst. Before each run the vessel was sealed and filled with 2 MPa N_2. After the reaction, the vessel was rapidly immersed into ice-bath. Similar procedures were followed for fructose dehydration in all solvents with the Hβ catalyst. The products of reaction were centrifuged for 5 min and then filtered to obtain a clear solution. The samples were analyzed by high-pressure liquid chromatography (HPLC, Agilent 1260) with a Shodex SH1821 Sugar capillary column (300 mm × 8 mm × 6 μm) and GC (Agilent 7890 A) with an AB-INNOWAX capillary column (30 m × 0.32 mm × 0.5 μm). Carbohydrates were detected with RI detector (RID). The mobile phase was 0.01 M H_2SO_4 flowing at a rate of

Scheme 1. Conversion of fructose in GBL and NMP; GBL: γ-butyrolactone, NMP: N-methyl-pyrrolidone.
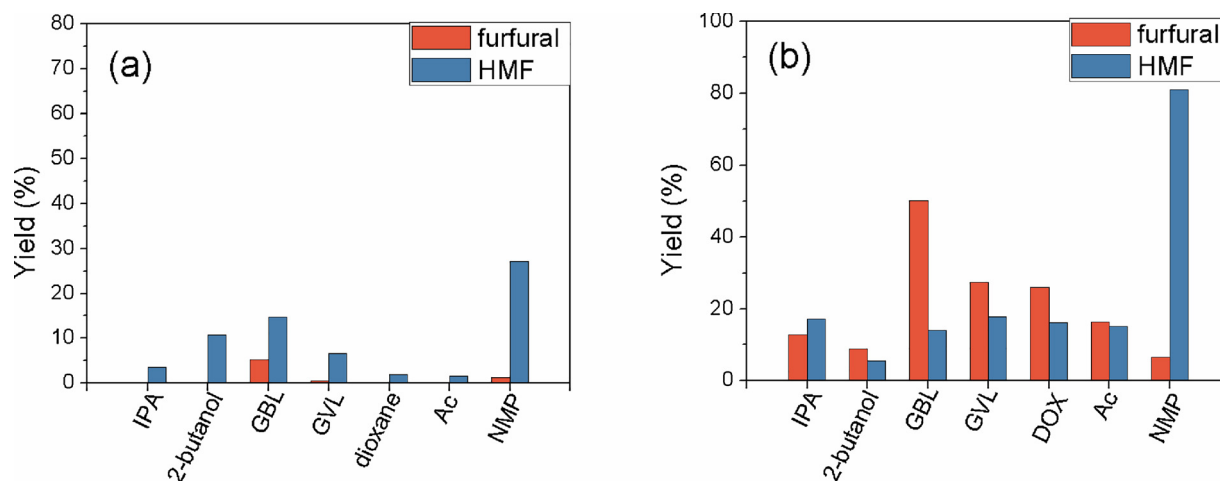
Fig. 1. HMF and furfural yield achieved by dehydration of fructose. (a) Reaction without catalyst in various solvents. (b) Reaction over Hβ zeolite under the same condition. *Reaction condition:* fructose (0.5 g), Hβ (0.1 g), solvent (9.5 g), 150 °C, 1 h. IPA: Isopropanol, DOX: 1,4-Dioxane, Ac: Acetone. All organic solvents contained 5 wt% H_2O.

0.6 m L/min. The standard solutions were used to obtain the calibration curves to calculate concentrations of the compounds by external standard method.

The conversion of substrate and the yield of products were quantified according to the following equations:

$$\text{Conversion (mole \%)} = \frac{\text{mole of sugar(inlet)} - \text{mole of sugar (outlet)}}{\text{mole of sugar (inlet)}} \times 100\%$$

$$\text{Yield (mole \%)} = \frac{\text{mole of one product produced}}{\text{mole of theoretical product value}} \times 100\%$$

2.3. Preparation of samples and catalyst characterization

The preparation of samples was based on the following procedure. 0.5 g Hβ zeolite was added in 9.5 g NMP or GBL. The mixture was stirred for 1 h at 150 °C. The solid sample was separated and then dried for 5 h on vacuum condition for NMR and XRD characterization.

The powder and adsorbed catalysts were analyzed by X-ray diffraction (XRD) in a BrukerAxs D2 diffractometer, using Cu *Kα* radiation from a Cu X-ray tube (λ = 0.154 nm) at 30 KV and 10 mA. Texture properties of the parent and adsorbed catalysts were determined by N_2 adsorption at 77 K in a Micromeritics ASAP 2420 surface analyzer. The micropore volume and surface area of the samples were obtained by BJH and BET method respectively.

The FTIR spectra of adsorbed pyridine were recorded on a Bruker VERTEX 70. Self supported wafers of the samples with a weight / surface ratio of about 20 mg/cm^2 were placed in a vacuum cell greaseless stopcocks and CaF_2 windows. The samples were evacuated at 350 °C for 30 min, exposed to pyridine vapour at room temperature for 20 min and then outgassed for 30 min at different temperatures (i.e. 200, 350 °C). We applied the extinction coefficients estimated form Take et al. to the integrated absorbance of 1543 cm^{-1} and 1453 cm^{-1} peaks in order to determine the ratio of Brönsted and Lewis acid density in the zeolite sample [38].

All solid-state magic-angle-spinning nuclear magnetic re (MAS NMR) measurements were performed on Bruker Avance III HD spectrometer (600 MHz, B_0 = 14.1 T) at a rotating frequency of 10 KHz at 25 °C.

For ^{27}Al MAS NMR, the unhydrated samples were packed into a 4 mm ZrO_2 rotor. The spectra were recorded at a resonance frequency of 156.4 MHz. The excitation pulse length was 0.40 µs, and the recycle time was 1 s. The chemical shifts were referenced to an external standard of $Al(NO_3)_3$ (δ = 0 ppm).

For ^{29}Si MAS NMR, the samples were packed into 4 mm ZrO_2 rotor. The spectra were recorded at a resonance frequency of 119.2 MHz. The pulse length was 2.0 µs, and the recycle time was 20 s. The chemical shifts were referenced to an external standard of kaolin (δ = -91.5 ppm).

Products analysis by Gas chromatography/Mass spectrometry (GC/MS) was further used to identify the C1 side product eliminated from fructose. The sample was analyzed by an Agilent G6890A series GC system connected to an Agilent G1530M quaternary pole mass detector, using electrospray ionization (EI) 70 eV in the positive mode. Released compounds were identified by comparison of their mass spectra with those contained within the NIST libraries, and the retention times and mass spectra of standards.

3. Results and discussions

3.1. Dehydration of fructose in different media

Initially, the major products from fructose in various organic solvents had been investigated with and without catalyst. The significant effect of solvents in the dehydration reaction of fructose had been confirmed. Although the presence of water is disadvantage for furfural production, a fraction of water is needed to solubilize the fructose. As *Cui* et al. [28] proposed that the presence of 5 wt % water was acceptable as furfural could still be obtained with high yields and rates. As shown in Fig. 1a, HMF was the main product in all the solvents by autocatalysis of the dehydration reaction without Hβ in spite of the little yields of furfural in GBL, GVL and NMP. However, in the presence of Hβ, the yield of furfural obviously increased in these solvents with exception of NMP (as show Fig. 1b). The various yield of furfural were achieved in lactones, ethers and ketones solvents may stem from the fact that the fructose and furfural was degraded *via* different ways and different extents in these solvents [35] (Table 1, Entries 1–7). The highest yield of furfural was obtained in lactones solvents such as GBL and GVL. Cui. et al. [28] pointed out that the arabinose (C_5) maybe is an important intermediate product for the transformation of C_6-sugars into furfural. The formation of arabinose in these solvents with exception NMP indicating that the furfural was effectively obtained *via* selective carbon-carbon bond cleavage over Hβ (Scheme 1).

Meanwhile, when GBL as solvent, the C1 side product coupling with C5 intermediate was identified as formaldehyde by gas chromatography/mass spectrometer (as shown in Fig. S1). This result indicated that the formation of furfural maybe was mainly ascribed to the retro-

Table 1
The conversion of fructose in various solvent over Hβ.[a]

Entry	Solvents[b]	Conv. (%)[c]	Selectivity (%)					
			Furfural	HMF	Glu	Ara	FA	LA
1	IPA	92.0(53)	13.86(8.3)	18.63(12)	1.74	4.17	2.84	3.04
2	2-butanol	99.9(55)	8.81(26)	5.51(24)	/	14.74	5.96	1.04
3	GBL	99.9(61)	50.25(44)	14.00(19)	1.94	5.27	3.39	5.58
4	GVL	99.9(47)	27.44(18)	17.80(14)	1.32	3.59	2.71	5.40
5	DOX	99.9(58)	25.94(24)	16.11(34)	1.77	3.38	5.10	7.54
6	Ac	98.0(57)	16.58(17)	15.36(8.7)	3.24	7.71	1.40	0.40
7	NMP	97.4(42)	6.73(2.7)	83.30(69)	2.2	/	0.79	0.23

[a] 0.1 g catalyst; 0.50 g fructose, 9.50 g solvent; 150 °C, 2 MPa N_2. Glu: glucose, Ara: arabinose, FA: formic acid, LA: levulinic acid, IPA: Isopropanol, DOX: 1,4-Dioxane, Ac: Acetone.
[b] Organic solvents contained 5 wt% H_2O.
[c] Intermediate conversion and corresponding selectivity were shown in bracket.

aldol reaction. The further mechanistic investigation will be carry out in next step. In addition, the furfural maybe was derived from HMF *via* eliminating hydroxymethyl group, this possible pathway has been ruled out in our reaction condition. The furfural was no detected when HMF as initial material in different reaction temperature (as shown in ESI†, Table S1). Furthermore, in order to direct comparison of selectivity, each reaction was allowed to proceed until the fructose conversion was ca. 50%. As shown in Table 1 bracket, used GBL as solvent, the furfural selectivity was also significant higher than other solvents at intermediate conversion. Notably, this tendency was retained at high conversion (ca. 99.9%). In addition, NMP achieved HMF selectivity about 69% at 42% conversion, which increased to 83% without degradation at high conversion. Additionally, the arabinose was no detected at intermediate conversion in all cases, indicating that the dehydration rate of C5 intermediate maybe was faster than the cleavage of carbon−⊕ carbon bond during the initial period of furfural formation.

Nevertheless, the overwhelming yield of HMF compared with furfural and the absent of arabinose should imply that the Hβ was inactive for the formation of furfural in NMP (Table 1, Entry 7). Meanwhile, as shown in Scheme 2, the observation of small amount glucose and furfural in NMP indicate that dehydration of fructose should take place *via* acyclic pathways in this solvent. The formation of furfural could be attributed to decarbonylation that competes with the final dehydration step to HMF [39]. These results suggest that the Hβ selectivity could be tuned *via* interaction between solvent molecular and active sites. On the basis of the experimental data, fructose may convert to different products *via* various routes due to synergistic effect between solvents and zeolite. Since the highest yield of furfural and HMF was obtained in GBL and HMF respectively, so the GBL and NMP was chosen as
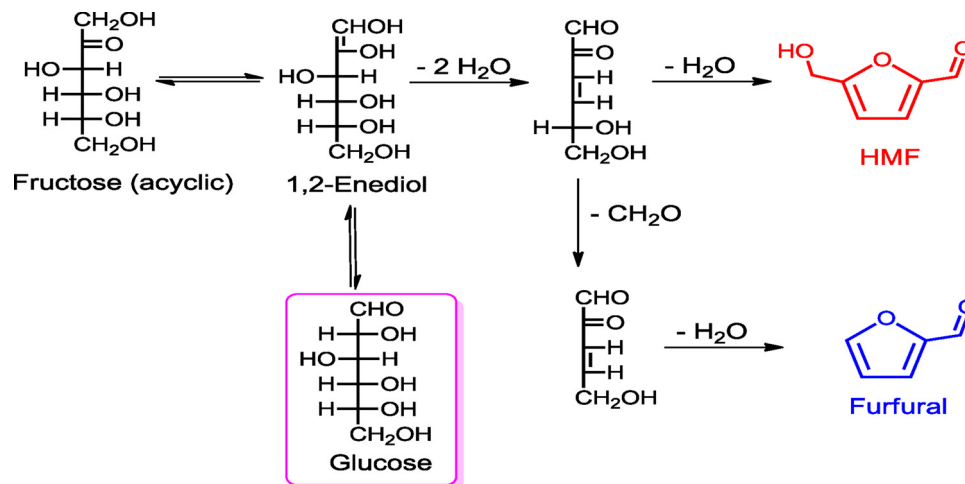
representation for investigating relationship between Hβ selectivity and solvent effects in the following section.

3.2. The effect of temperature on the selectivity of catalyst

The effect of the reaction temperature on the selectivity of Hβ was further investigated from 100 to 160 °C. As evidenced by Fig. 2, a negligible effect of reaction temperature on the Hβ selectivity in GBL and NMP was observed. Here, we defined selectivity as a ratio of yield and the value of ratio exceeded 1:1 represent the furfural or HMF was a predominant product. With temperature gradually increasing, the selectivity tendency of furfural and HMF was maintained in spite of the diverse yield were obtained in different reaction temperature. Additionally, the selectivity of furfural was slightly increased in all temperature range also indicated that the formation of furfural not was strong depended on the configuration of aluminum but on the pore structure of Hβ. In contrast, the selectivity of HMF was significant increased at elevated temperature implied that the acid active sites and coordinated environment of aluminum was mainly responsible for higher selectivity of HMF. Finally, higher temperature led to a slight decrease of product yield duo to the formation of humus. These results also indicated that the reverse selectivity of Hβ only originated from the interplay between solvent and zeolite.

3.3. Interaction between NMP and Hβ

Solid state magic angle spinning (MAS) unclear magnetic resonance (NMR) was an excellent technique to probe the local environment of silicon and aluminum species. To understand the underlying reasons,

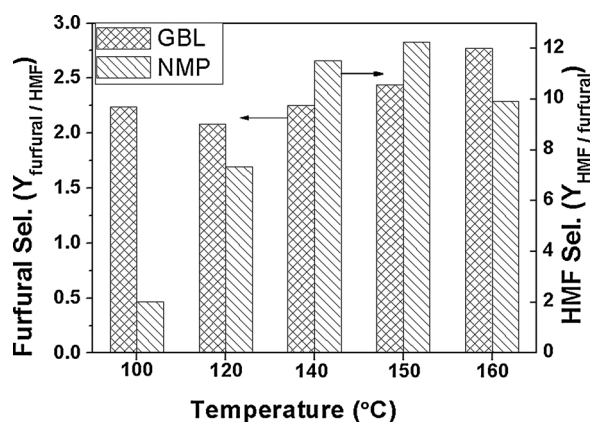**Scheme 2.** Formation of furfural and glucose from fructose in NMP [40].

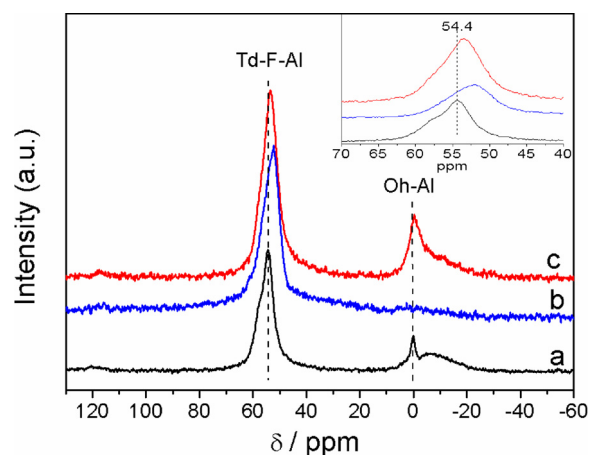**Fig. 2.** The effect of temperature on selectivity in GBL and NMP.

Fig. 3. The ^{27}Al MASNMR spectrum of samples; a) parent Hβ, b) interplay with NMP, c) interplay with GBL.

^{29}Si and ^{27}Al MAS NMR was carried out to investigate the interaction between solvent molecular and zeolite active sites. In ^{27}Al MAS NMR, several reasons for shifts in peak position exist. The peak position is related to (i) the coordination number, (ii) the Al-O-Si angle, (iii) the mean Al-O distance and (iv) the presence of quadrupolar interactions [41]. As shown in Fig. 3, peak at 54.4 ppm could be ascribed to the overlapping tetrahedrally coordinated framework aluminum (Td-F-Al) [42]. The resonance peak around 0 ppm is a superposition of sharp peak assigned to well-ordered octahedrally coordinated aluminum (Oh-Al) species, while the broad peak at – 6 ppm is assigned to Oh-Al species in more distorted environment [43,44]. The alteration of chemical shifts provides evidence of an interaction between the solvent molecular and zeolite (Fig. 3, inset). Here, the slight alteration of Td-F-Al resonance peak may be due to a variation in Al-O-Si bond angle [45]. Generally, the width of resonance peak reflects symmetry around the Al atoms. Upon interaction of GBL on Hβ, the single broad resonance peak at 0 ppm suggests that the distorted Oh-Al convert to more well-order. But the local symmetry of Oh-Al atoms became lower than before interplay of GBL. Remarkably, the distinctly difference is that the disappearance of Oh-Al resonance peak duo to introduction of NMP molecular. The disappearance of Oh-Al resonance suggested that the NMP display stronger interaction with Oh-Al sites than GBL. Two possible reasons for disappearance of the Oh-Al resonance peak have been proposed. Specifically, one possibility is that the disappearance of the peak near 0 ppm could result from the loss of H$_2$O or OH groups in zeolite lattice during dehydration [46]. The other is that Oh-Al can be reversibly converted into Td-Al by adsorption of organic bases such as gaseous ammonia or a solution of pyridine [47].
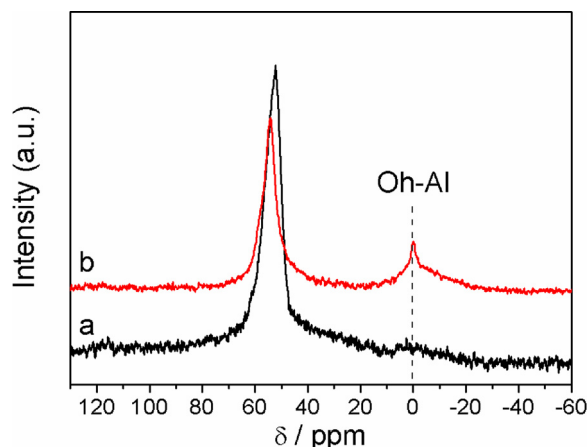

Fig. 4. ^{27}Al MASNMR spectrum of Hβ zeolite; a) interplay with NMP, b) calcination of sample (treated by NMP). (For interpretation of the references to colour in this figure legend, the reader is referred to the web version of this article.)

The first reason could be ruled out because of that the absorption procedures zeolite have not been further calcined. The thermal treatment was performed in order to confirm the second possible reason. The sample interacted with NMP was calcined at 500 °C for 3 h, as shown in Fig. 4, the peak of Oh-Al at 0 ppm was generated again, corresponding well with observation of Bourgeat-Lami et al. [47]. Therefore, these observations apparently indicated that the disappearance of Oh-Al resonance peak should result from reversibly conversion of Oh-Al into Td-Al when NMP was introduced into zeolite acid sites.

Currently, there are two attitudes to the assignment of the relatively sharp resonance peak near 0 ppm in the previous reports [44,48,49]. One proposes it could be ascribed to the octahedrally coordinated framework aluminum (Oh-F-Al) duo to partial breakage of the Si-O-Al bond and the other attributes it to octahedrally coordinated extra-framework aluminum (Oh-EF-Al) duo to dealumination [50,51]. However, the coordinated environment of framework silicon should be changed, if Oh-EF-Al was reinserted in framework sites. Therefore, ^{29}Si MASNMR was performed in order to distinguish the assignment of Oh-Al sits. As shown in Fig. 5, the unstrained spectrum indicating that there are no changes in the environments of the silicon atoms. It could be inferred that the Oh-Al might constitute inherent parts of the zeolite framework linked to four lattice oxygens, the oxygen of a hydronium ion, and the oxygen of a water molecular [47,52]. It could be concluded that the Al^{IV}-Al^{VI} transformation is totally reversible since solvent
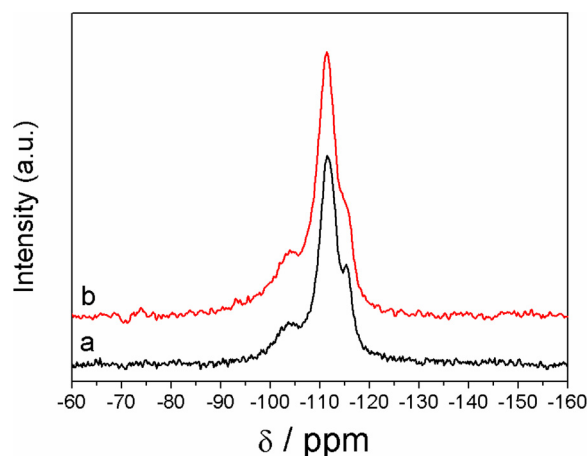

Fig. 5. ^{29}Si MASNMR spectra of samples; a) parent Hβ, b) interplay with NMP.

interaction allows for all the aluminum atoms to recover a tetrahedral configuration, which in turn influenced the Hβ selectivity. Accordingly, the dehydration reaction preferred in NMP allows the fructose effectively transform into HMF at the Td-F-Al sites. It is widely accepted that only Td-F-Al generates Brønsted acid site (BAS) in the zeolites [48]. Thus, the fructose was compelled to completely consume on Td-F-Al active sites and a high yield of HMF could be obtained *via* acyclic pathway. As exhibited above, the considerable yield of furfural was obtained in GBL. This also indicated that Oh-F-Al may be the main active site for the selective cleavage of carbon-carbon bond.

3.4. The effect of GBL for furfural production

Based on the aforementioned data, the furfural was always predominant product in non-amides solvents and the higher yield was achieved in GBL. Especially, the intrinsic reason need to be further investigated, which the highest yield of furfural was obtained in GBL. The configuration of aluminum was not converted after treated by GBL. Hence, some other important factors also were able to enhance the selectivity of Hβ for production of furfural. It is a widely accepted fact that the presence of carbonyl group allows furfural to be degraded easily over acid solid catalysts (Hβ zeolite) through aldol condensation reaction. However, the extent of degradation could be alleviated by solvent effects. Therefore, the degradation of furfural was also investigated in different reaction media. Here, the extent of degradation was defined as degraded mole of furfural divide by initial mole of furfural. The higher the number is, the more furfural was degraded. It can be seen in Fig. 6, the most amount of furfural was degraded in acetone, followed by alcohols solvents. Therefore, the lower yield of furfural was obtained in these solvents accorded with the extent of degradation. Although the negligible degradation was observed in GBL and dioxane, the higher yield of furfural was achieved in GBL. These results indicated that the GBL play an important role for formation of furfural comparing with dioxane.

In order to deeply investigate the effect of GBL, the turnover frequency (TOF) values for fructose conversion were determined in GBL and dioxane using Hβ as catalyst. As shows in Table 2, the use of GBL as a solvent increase the TOF by 2.12 times compared to the value obtained when dioxane is used as the solvent.

This behavior allows us to describe the increase in reaction rates (TOF$_{GBL}$ / TOF$_{DOX}$) for acid catalyst of differing strengths in GBL compared to reaction carried out in dioxane. Therefore, the increases in value of TOF and the suppression of degraded reaction may be responsible for the higher yield of furfural when the reaction was carried out in GBL.
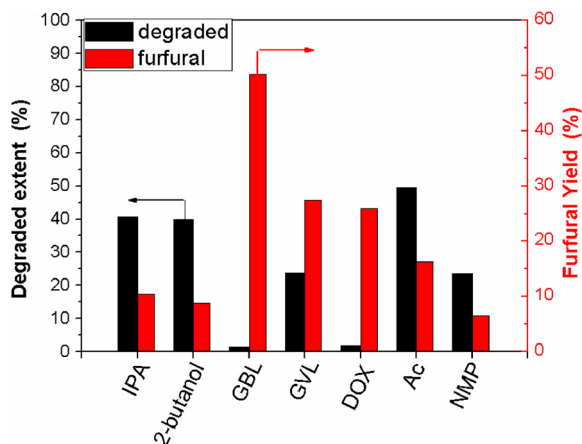

Fig. 6. The extent of degraded in different solvent; IPA: isopropanol, DOX: dioxane, Ac: acetone.

Table 2
Turnover frequency (TOF) for the conversion of fructose to furfural.[a]

Solvents[b]	Catalyst	T / °C	TOF / min^{-1}
GBL	Hβ	150	17.4
Dioxane	Hβ	150	8.2

[a] Reaction condition: 1.70 wt% (satuated solubility) fructose, solvent (10 g).
[b] Solvents contained 5 wt% H$_2$O, a fraction of water is needed to solubilize the fructose.

3.5. Nature of acid sites studied by FT-IR spectroscopy

The relationship between nature of acid sites and configuration number of aluminum was investigated by FT-IR observation employing pyridine as probe molecule. The determination of FT-IR was impeded because of the octahedrally coordinated aluminum was generated again during desorption procedure at high temperature condition (350 °C). In addition, the real density of acid sites could not be easily determined duo to the residual of NMP molecule. In order to overcome this problem, the ionexchange procedure was performed for transformation of octahedrally coordinated aluminum [47]. For this test, 0.5 g Hβ was stirred in 0.5 mol/L potassium nitrate solution for 4 h at 80 °C. The catalyst was washed three times with water and dried on vacuum condition at 80 °C for 6 h. All aluminum atoms were detected by ^{27}Al MAS NMR in the ion-exchanged sample. They were all located in a tetrahedral configuration when the compensating cation was a potassium ion (as shown in Fig. S2). Upon pyridine adsorption new adsorption bands appears at 1544 cm^{-1} and 1454 cm^{-1}, which are ascribed to the interaction of pyridine with strong Brønsted and Lewis acid sites, respectively (as shown in Fig. S3). The amount of adsorbed pyridine after evacuation at 200 °C is summarized in Table 3. The amount of adsorbed pyridine on Brønsted and Lewis acid sites (BAS and LAS) of parent Hβ were 0.28 and 0.17 mmol/g, respectively. As the ion-exchange was carried out, the concentrations of BAS and LAS are 0.033 and 0.057 mmol/g (Table 3), respectively, indicating that ionexchange does not remove all acid sites in this sample that are available for interaction with pyridine. Namely, the ratio of BAS to LAS (B/L ratio) was decreased from 1.65 to 0.59. These results suggest that the BAS was prior exchanged, corresponding with the observation of previous report [53]. However, the decrease of LAS may be arises from the modulation of aluminum coordinated environment. It is worth note that the ionexchange is essential different from the interaction between NMP and Hβ for density of acid sites. The high yield of HMF was obtained in NMP, indicating that the density of BAS may not be sharply decreased with exception of transforming coordinated environment.

The effect of the Al^{IV}-Al^{VI} transformation after ion-exchange on the dehydration activity and selectivity is also shown in Table 3. Despite the total yield of furfural and HMF was decline about 23% due to decrease of BSA, the major products also were reversed in line with transformation of octahedrally configuration. The HMF also was a main product under the same reaction condition, corresponding with the observation of NMP. These results clearly indicated that the formation

Table 3
Adsorbed pyridine after desorption at 200 °C.[a]

Entry	Catal.	Conv. (%)[b]	Yield (%)		Acid sites density (mmol/g)		
			Furfural	HMF	Brønsted	Lewis	B/L
1	Hβ	99.9	50.25	14.00	0.28	0.17	1.65
2[c]	KHβ	90.0	13.12	28.00	0.033	0.057	0.59

[a] each acid amount was calculated by using the reported molar extinction coefficient in Ref. [38].
[b] 0.5 g fructose, 9.5 g GBL, 0.1 g catalyst, 150 °C, 2 MPa N$_2$.
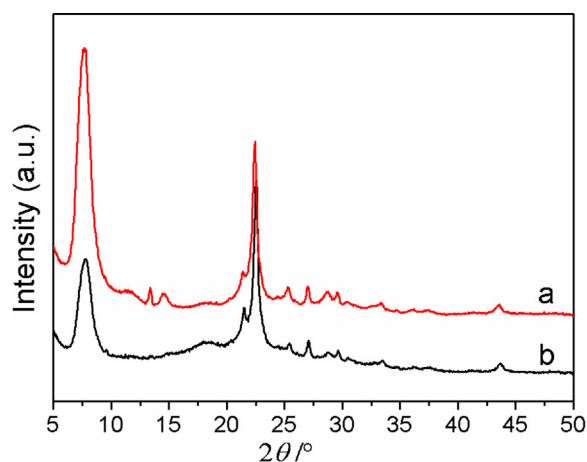[c] the ion-exchanged Hβ zeolite.

Fig. 7. The experimental powder XRD patterns of a) parent Hβ, b) NMP treated Hβ.

Table 4
Dehydration of fructose in other amide solvents.[a]

Entry	Solvent	Catal.	Conv. %	Yield %				
				HMF	Furfural	Ara	Glu	LA + FA
1	DMA	Hβ	74.6	46.3	3.78	/	/	0.63
2[b]	DMI	Hβ	95.44	89.72	2.93	/	1.87	0.11
3[c]	DMA	/	47.2	16.54	3.41	/	/	2.01
4[b,c]	DMI	/	11.2	6.54	/	/	/	0.45

Ara: arabinose, Glu: glucose, DMA: dimethylacetamide, DMI: 1,3-dimethyl-2-imidazolidinone.
[a] 0.5 g fructose; 0.1 g catalyst, 9.5 g solvent, 150 °C, 1 h, 2 MPa N_2.
[b] 0.5 g fructose; 0.1 g catalyst, 9.5 g solvent, 130 °C, 1 h, 2 MPa N_2.
[c] The reaction was carried out without catalyst.

of furfural from fructose *via* selective carbon-carbon bond cleavage should need an appropriate configuration environment of aluminum. This further confirmed that the selectivity of Hβ was reversed by modulation of framework aluminum coordination number, inducing by interaction between NMP and Hβ.

3.6. Structural propeties of catalysts

X-ray diffraction (XRD) and BET were also conducted to understand the effect of solvents on the structure of Hβ. As shown in Fig. 7, the diffraction peaks located at $2\theta = 7.6°$ and $22.4°$ could be attributed to typical Hβ (JCPDS: 47-0183) [54–56]. Noteworthily, the decline of diffraction peak at $2\theta = 7.6°$ should result from the demonstrated interaction between NMP and Hβ. Compared with parent Hβ zeolite, almost unstrained XRD profiles indicated that their lattice structure was maintained after the modification of coordinated environment aluminum induced by interaction of solvent.

This was also consistent with the observation from BET characterization (shown in Table S2 and Fig. S4). The parallel N_2 adsorption/desorption isotherms and pore volume clearly suggested that the pore structure of the Hβ was scarcely changed with modification of coordinated environments of aluminum. The NMP deposited on the surface of zeolite, resulting in the decrease in the surface area and pore volume of the samples. By employing XRD and BET complementary characterization methods, we further confirmed that the reversible alteration of selectivity only result from the transformation of coordinated environment aluminum.

3.7. Performance of Hβ in other amide solvents

Moreover, other amide solvents such as dimethylacetamide (DMA) and 1,3-dimethyl-2-imidazo-lidinone (DMI) were also introduced in the dehydration of fructose over Hβ. As showed in Table 4, HMF also was the predominated product in DMA and DMI under the optimal condition, corresponding with the observation in NMP. In addition, the ^{27}Al MAS NMR spectrum indicated that DMA and DMI molecular could also induce the reversibly conversion of Oh-F-Al into Td-F-Al (as shown in the Fig. S5).

This should further demonstrate that the transformation of octahedral framework aluminum configured in Hβ was results from the interaction between zeolite and amide molecular. The alteration of the framework aluminum would lead to different distribution of the major products for fructose dehydration reaction.

4. Conclusion

This paper presents solvent-dependent products distribution of the Hβ catalyzed dehydration reaction. Strong solvent effects appeared on the selectivity of reaction in the dehydration of fructose using Hβ catalyst. Moreover, a favourable yield of 50.25% for furfural can be achieved, owing to the TOF value was enhanced and the degradation of furfural was suppressed in GBL. When the reaction carried out in NMP under the same condition, the HMF yield for converting fructose reached 81.14%. The intrinsic reason of solvent effects is the modulation of the coordinated environment aluminum induced by interplay between solvents and Hβ active sites. In the ^{27}Al MAS NMR spectrum, aluminum species are detected from which the coordination can be reversibly changed from a 6-fold state to tetrahedrally coordinated species by means of introducing amide solvents. The modulation of coordination number in turn influenced the selectivity of Hβ. Therefore, the amide solvents, such as NMP, DMA and DMI, give a higher selectivity to HMF. In contrast, the lactones solvents (GBL) exhibit a higher selectivity to furfural. Our results suggest that the strong interaction between solvents and Hβ zeolite has a crucial influence on the catalytic performance, and then bring forward an effective approach to improving the selectivity by regulating the solvents.

Acknowledgements

Appendix A. Supplementary data

Supplementary material related to this article can be found, in the online version, at doi:https://doi.org/10.1016/j.apcatb.2018.04.043.

References

[1] J.A. Melero, J. Iglesias, A. Garcia, Energy Environ. Sci. 5 (2012) 7393–7420.
[2] R. Karinen, K. Vilonen, M. Niemela, ChemSusChem 4 (2011) 1002–1016.
[3] J. Lessard, J.-F. Morin, J.-F. Wehrung, D. Magnin, E. Chornet, Top. Catal. 53 (2010) 1231–1234.
[4] E.I. Gurbuz, J.M. Gallo, D.M. Alonso, S.G. Wettstein, W.Y. Lim, J.A. Dumesic, Angew. Chem. Int. Ed. 52 (2013) 1270–1274.
[5] W. Mamo, Y. Chebude, C. Márquez-Álvarez, I. Díaz, E. Sastre, Catal. Sci. Technol. (2016) 2766–2774.
[6] E. Nikolla, Y. Román-Leshkov, M. Moliner, M.E. Davis, ACS Catal. 1 (2011) 408–410.
[7] X. Qi, M. Watanabe, T.M. Aida, J.R.L. Smith, Green Chem. 11 (2009) 1327–1331.
[8] X. Qi, M. Watanabe, T.M. Aida, J.R.L. Smith, Green Chem. 10 (2008) 799–805.
[9] Z. Huang, W. Pan, H. Zhou, F. Qin, H. Xu, W. Shen, ChemSusChem 6 (2013) 1063–1069.
[10] M. Cheng, T. Shi, H. Guan, S. Wang, X. Wang, Z. Jiang, Appl. Catal. B: Environ. 107 (2011) 104–109.
[11] A.S. Dias, M. Pillinger, A.A. Valente, Microporous Mesoporous Mater. 94 (2006) 214–225.
[12] Y. Zhang, V. Degirmenci, C. Li, E.J. Hensen, ChemSusChem 4 (2011) 59–64.

[13] C.H. Kuo, A.S. Poyraz, L. Jin, Y. Meng, L. Pahalagedara, S.Y. Chen, D.A. Kriz, C. Guild, A. Gudz, S.L. Suib, Green Chem. 16 (2014) 785–791.

[14] A.S. Luqman Atanda, Swathi Mukundan, Qing Ma, Muxina Konarova, Jorge Beltramini, ChemSusChem 8 (2015) 2907–2916.

[15] H.T. Kreissl, K. Nakagawa, Y.K. Peng, Y. Koito, J. Zheng, S.C.E. Tsang, J. Catal. 338 (2016) 329–339.

[16] S. Mondal, J. Mondal, A. Bhaumik, ChemCatChem 7 (2015) 3570–3578.

[17] Q.-Y. Liu, F. Yang, Z.-H. Liu, G. Li, J. Ind. Eng. Chem. 26 (2015) 46–54.

[18] M.W. Xinhua Qi, Taku M. Aida, Richard Lee Smith Jr., Ind. Eng. Chem. Res. 47 (2008) 9234–9239.

[19] A. Dibenedetto, M. Aresta, L. di Bitonto, C. Pastore, ChemSusChem 9 (2016) 118–125.

[20] J. Zhou, Z. Xia, T. Huang, P. Yan, W. Xu, Z. Xu, J. Wang, Z.C. Zhang, Green Chem. 17 (2015) 4206–4216.

[21] M.J. Climent, A. Corma, S. Iborra, Green Chem. 13 (2011) 520–540.

[22] A.S. Mamman, J.M. Lee, Y.C. Kim, I.T. Hwang, N.J. Park, Y.K. Hwang, J.S. Chang, J.S. Hwang, Biofuels, Bioprod. Bior. 2 (2008) 438–454.

[23] S. Caratzoulas, M.E. Davis, R.J. Gorte, R. Gounder, R.F. Lobo, V. Nikolakis, S.I. Sandler, M.A. Snyder, M. Tsapatsis, D.G. Vlachos, J. Phys. Chem. C 118 (2014) 22815–22833.

[24] A.A. Rosatella, S.P. Simeonov, R.F.M. Frade, C.A.M. Afonso, Green Chem. 13 (2011) 754.

[25] S.M. Bruce, Z. Zong, A. Chatzidimitriou, L.E. Avci, J.Q. Bond, M.A. Carreon, S.G. Wettstein, J. Mol. Catal. A: Chem. 422 (2016) 18–22.

[26] J.A.M. Jose Iglesias, Gabriel Morales, Marta Paniagua, and BlancaHernndez, ChemCatChem 8 (2016) 2089–2099.

[27] J.M.R. Gallo, D.M. Alonso, M.A. Mellmer, J.H. Yeap, H.C. Wong, J.A. Dumesic, Top. Catal. 56 (2013) 1775–1781.

[28] J. Cui, J. Tan, T. Deng, X. Cui, Y. Zhu, Y. Li, Green Chem. 18 (2016) 1619–1624.

[29] J. Jae, G.A. Tompsett, A.J. Foster, K.D. Hammond, S.M. Auerbach, R.F. Lobo, G.W. Huber, J. Catal. 279 (2011) 257–268.

[30] A. Zheng, B. Han, B. Li, S.B. Liu, F. Deng, Chem. Comm. 48 (2012) 6936.

[31] H. Yoshida, Y. Onodera, S.-I. Fujita, H. Kawamori, M. Arai, Green Chem. 17 (2015) 1877–1883.

[32] B. Karimi, H.M. Mirzaei, H. Behzadnia, H. Vali, A.C.S. Appl, Mater. Inter. 7 (2015) 19050–19059.

[33] H.M. Chase, T.J. McDonough, K.R. Overly, C.M. Laperle, J. Phys. Org. Chem. 26 (2013) 322–326.

[34] M.A. Mellmer, C. Sener, J.M. Gallo, J.S. Luterbacher, D.M. Alonso, J.A. Dumesic,

Angew. Chem. Int. Ed. 53 (2014) 11872–11875.

[35] X. Hu, R.J.M. Westerhof, D. Dong, L. Wu, C.-Z. Li, A.C.S. Sustain, Chem. Eng. 2 (2014) 2562–2575.

[36] X. Wang, R. Rinaldi, ChemSusChem 5 (2012) 1455–1466.

[37] V.V. Ordomsky, J. van der Schaaf, J.C. Schouten, T.A. Nijhuis, J. Catal. 287 (2012) 68–75.

[38] T.Y.J. Take, K. Miyamoto, H. Ohyama, M. Misono, Stud. Surf. Sci. Catal. 28 (1986).

[39] R.D.S.R.J.D. Claude Moreau, Pierre Faugeras, Patrick Rivalier, Pierre Ros, Gerard Avignon, Appl. Catal. A: Gen. 145 (1996) 211–224.

[40] R.J. van Putten, J.C. van der Waal, E. de Jong, C.B. Rasrendra, H.J. Heeres, J.G. de Vries, Chem. Rev. 113 (2013) 1499–1597.

[41] A.P.M. Kentgens, Geoderma 80 (1997) 271–306.

[42] P. Sazama, E. Tabor, P. Klein, B. Wichterlova, S. Sklenak, L. Mokrzycki, V. Pashkkova, M. Ogura, J. Dedecek, J. Catal. 333 (2016) 102–114.

[43] A.J.Av.B. Beers, K.M. de Lathouder, F. Kapteijn, J.A. Moulijn, J. Catal. 218 (2003) 239–248.

[44] S.M. Maier, A. Jentys, J.A. Lercher, J. Phys. Chem. C 115 (2011) 8005–8013.

[45] A.L.R.J.A. van Bokhoven, D.C. Koningsberger, J. Phys. Chem. B 104 (2000) 6743–6754.

[46] Z. Zhao, S. Xu, M.Y. Hu, X. Bao, C.H.F. Peden, J. Hu, J. Phys. Chem. C 119 (2015) 1410–1417.

[47] P.M. Elodie Bourgeat-Lami, Francesco Di Renzo, Pierre Espiau, F. Fajula, Appl. Catal. 72 (1991) 139–152.

[48] C.C.-F.R.A. Beyerlein, J.B. Hall, B.J. Huggins, G.J. Ray, Top. Catal. 4 (1997) 27–42.

[49] H.K.C.T. Guenter, H. Kuehl, Microporous Mesoporous Mater. 35–36 (2000) 521–532.

[50] B.J.Z.P.J. Kunkeler, J.C. van derWaal, J.A. van Bokhoven, D.C. Koningsberger, H. van Bekkum, J. Catal. 180 (1998) 234–244.

[51] R. Otomo, T. Yokoi, J.N. Kondo, T. Tatsumi, Appl. Catal. A: Gen. 470 (2014) 318–326.

[52] T.H.C.B.H. Wouters, P.J. Grobet, J. Am. Chem. Soc. 120 (1998) 11419–11425.

[53] O. Kikhtyanin, R. Bulánek, K. Frolich, J. Čejka, D. Kubička, J. Mol. Catal. A: Chem. 424 (2016) 358–368.

[54] J.S. Bin Xie, Limin Ren, Yanyan Ji, Jixue Li, F.S. Xiao, Chem. Mater. 20 (2008) 4533–4535.

[55] M.M.J.T.J.M. Newasm, W.T. Koeteier, C.B. de Gruyter, Proc. R.Soc. Lond. A 420 (1988) 375–405.

[56] R.B.L.J.B. Higgins, J.L. Schlenker, A.C. Rohrman, J.D. Wood, G.T. Kerr, W.J. Rohrbaugh, Zeolites 8 (1988) 446–452.